Available online at www.sciencedirect.com

Cement and Concrete Research 35 (2005) 1438–1446

Electrical conductivity and phase composition of calcium aluminate cement containing air-cooled and water-cooled slag at 20, 40 and 60 °C

M. Heikal[a,*], M.S. Morsy[b], M.M. Radwan[c]

[a]*Chemistry Department, Faculty of Science, Zagazig University, Benha Branch, Benha, Egypt*
[b]*Building Physics Department, Building Research Center, PO Box 1770, Cairo, Egypt*
[c]*National Research Center, Dokki, Cairo, Egypt*

Received 23 June 2003; accepted 23 September 2004

Abstract

Calcium aluminate cement (CAC) pastes containing Egyptian air-cooled slag (AS) or water-cooled slag (WS) were prepared using different amounts of slag, namely, 5, 10, 15, 20 and 25 mass%. The pastes were prepared with deionized water using the required water of standard consistency to produce normal workability. The variations of electrical conductivity with the hydration time were measured at 20, 40 and 60 °C. The results demonstrate that electrical conductivity is a useful technique to study the change in the phase composition at different temperatures during the setting and hardening of calcium aluminate cement as well as reflecting the role of AS and WS, preventing the conversion occurring during the CAC hydration.

Keywords: Calcium aluminate cement; Air-cooled slag; Water-cooled slag; Temperature; Electrical properties and microstructure

1. Introduction

Calcium aluminate cement (CAC) is very resistant to chemical attack and high temperatures. The temperature at which hydrates are formed is important in the hydration of CAC. Different hydration products are created, i.e., CAH_{10}, C_2AH_8 and C_3AH_6, depending on the temperature at which the process takes place. The conversion of hexagonal phases (CAH_{10} or C_2AH_8) to C_3AH_6 and AH_3 in the hydration of CAC under certain temperature conditions has been a major problem, limiting its use as a structural material. This conversion reduces the strength development of CAC.

Pure gehlenite does not seem to react with water, but the phase present in CAC contains other oxides in solid solution, and there is evidence that it is more reactive [1]. The presence of gehlenite hydrate (C_2ASH_8), also called stratlingite, in CAC pastes has been studied [2,3]. Stratlingite is an Afm phase closely related to C_2AH_8; it is stable relative to hydrogarnet at ambient temperature. The formation of stratlingite prevents the conversion of the hydration products of CAC [4]. It has also been shown that stratlingite forms as a stable phase in the temperature range of 20–70 °C [5]. It was reported that, in CAC-blends containing 30–50 mass% silica fume, stratlingite is the dominant hydration product after 1 week at 40 °C or below, but at higher temperatures, C_3AH_6 is already formed after 1 day. Microsilica and granulated blast-furnace slag can react with CAC in the presence of water, resulting in the formation of stratlingite [6,7]. Fentiman et al. [8] found that stratlingite was formed as the dominant hydrate when hydration occurs at 40 °C or above in mixtures containing around 50 mass% slag. At early ages, the strengths of 50:50 CAC/slag mixtures are lower than that of CAC alone. However, the blends show continuous increase in strength up to 2 years without a minimum in strength associated as a result of the conversion process.

Electrical conductivity and pH measurements conducted on dilute cement suspensions as a function of time indicated that the hydration of CAC is a dissolution and precipitation process [9–11]. Classical techniques such as XRD, DTA and SEM and advanced techniques (ultrasonic velocity, acoustic emission monitoring) were used to give informa-

---

* Corresponding author. Tel./Fax: +2 013 3222578.
E-mail address: ayaheikal@hotmail.com (M. Heikal).

0008-8846/$ - see front matter © 2004 Elsevier Ltd. All rights reserved.
doi:10.1016/j.cemconres.2004.09.027

Table 1
Chemical analysis of the starting materials, (mass%)

Oxides	CAC	AS	WS
SiO_2	4.59	32.69	37.21
Al_2O_3	53.68	8.17	10.45
Fe_2O_3	1.24	1.89	1.27
CaO	35.52	33.57	35.70
MgO	n.d.	1.35	2.05
SO_3	n.d.	0.01	0.15
L.O.I	n.d.	–	–
K_2O	n.d.	0.43	0.71
Na_2O	n.d.	1.47	1.60
TiO_2	2.92	0.46	0.35
MnO	Nill	4.48	3.50
BaO	–	6.63	3.11
S^-	Nill	0.01	3.62
Blaine surface area, cm^2/g	3500	3500	3200

tion about the morphology and phase composition of the formed hydrates [12,13].

Cement containing water-cooled slag (WS) has long been used in Egypt. However, there are many other unexploited slag by-products such as air-cooled blast furnace slag (BFS) and steel-making slag. The feasibility of utilizing these types of slags with cement has been ignored due to the judgment that air-cooled slag (AS) is hydraulically unreactive. Consequently, little of these materials is used, or their use is limited to low-value applications. A comparative study of the hydraulic reactivity of AS and WS produced from the same blast furnace and the same raw materials has been conducted [14]. Although the reactivity of AS is lower than WS at room temperature, it can still be exploited as a hydraulic material. Even, if these slags cannot fulfill the requirements of the standard specifications for blended cements, their hydraulic activities can be exploited in building materials such as autoclaved products or bricks. The latter may be an economical alternative for developing countries inasmuch as little technology is required.

The aim of this research work is to study the methods by which each type of slag mixed with calcium aluminate cement can be evaluated at 20, 40 and 60 °C curing temperatures. In the present study, electrical conductivity technique was used for monitoring the changes occurring during the initial setting from zero time (3 min) up to 7 days (10080 min) as well as for assessing the hydraulic activity of AS in comparison with WS. This investigation was carried out using pastes to correlate the physicochemical and microstructure characteristics of the hydration products which are formed.

Table 2
Mix compositions and the required water for normal consistency of CAC/slag blends

	CAC	AS	WS	Water of consistency, %
M.0	100	0	–	25.5
M.5	95	5	–	24.9
M.10	90	10	–	24.5
M.15	85	15	–	24.3
M.20	80	20	–	24.0
M.25	75	25	–	23.8
C.5	95	–	5	25.2
C.10	90	–	10	24.9
C.15	85	–	15	24.6
C.20	80	–	20	24.3
C.25	75	–	25	24.0

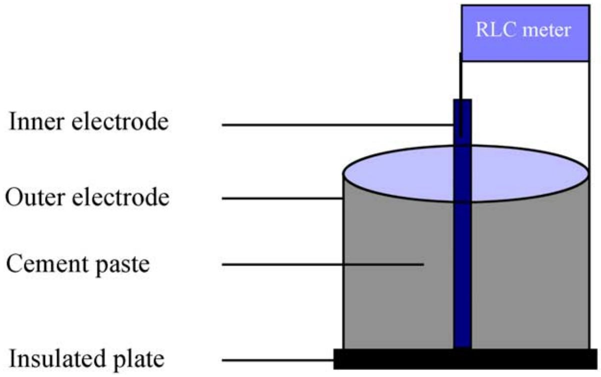

Fig. 1. Electrical conductivity cell.

2. Experimental techniques

The materials used in this investigation were calcium aluminate cement, Egyptian air-cooled and water-cooled slags provided by the Iron and Steel Company, Helwan, Egypt. The chemical composition of these raw materials is given in Table 1. XRD pattern of air-cooled slag reveals the presence of gehlenite (C_2AS) and quartz. The quartz may be contamination during the cooling process of molten slag. The water-cooled slag shows a hump existing between 20°–35°, indicating the presence of amorphous glassy phase. The mix proportions are shown in Table 2. Each blend was mixed in a porcelain ball mill with four balls for 1 h to

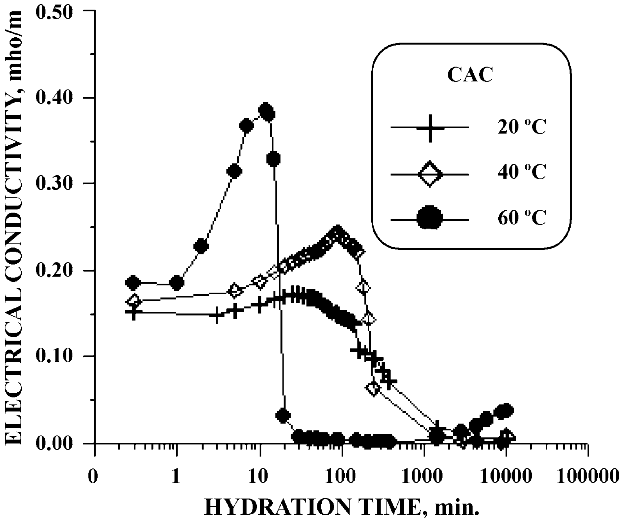

Fig. 2. Electrical conductivity of CAC at different temperatures.

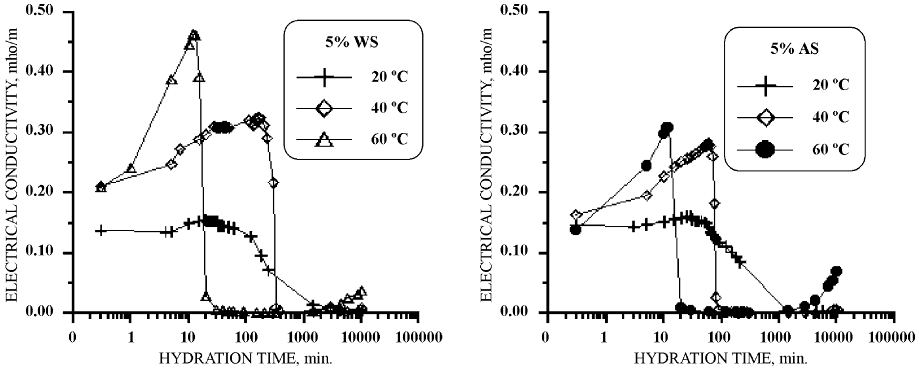

Fig. 3. Electrical conductivity of CAC containing 5 mass% of AS or WS at different temperatures.

assure complete homogeneity. The CAC was partially substituted by 5, 10, 15, 20 and 25 mass% of air-cooled or water-cooled slags. Different mixes were mixed with the required water of normal consistency given in Table 2.

The mixing water was poured on the cement and mixed for 3 min using a trowel and directly poured into 1-in. cubic moulds and pressed until homogenous specimens were obtained. The moulds were manually vibrated to remove any air bubbles, and the surface was smoothed by spatula. The moulds were cured in a humidity chamber at 100% relative humidity at 20 °C for the first 24 h, then demoulded and cured under water up to 60 days at three thermostatically controlled temperatures: 20, 40 and 60 °C.

In electrical conductivity measurements, the test cell was of the coaxial type and included concentric inner and outer electrodes mounted on an insulated base plate, as shown in Fig. 1. The electrodes were polished before the experiment [15]. The mixing was done with the required amount of water that gives normal consistency. The measurements of the electrical conductivity were begun exactly 3 min after mixing with water (zero time). The cement pastes were placed in the space between the electrodes. The cell was kept in a cabinet chamber at 100% relative humidity during the test period from 3 min up to 7 days (10,080 min). The electrical conductivity was measured at three different temperatures: 20, 40 and 60 °C. The electrodes were connected with RLC meter, model SR 720. All data on the electrical conductivity were measured during the setting and hardening at relativity low AC frequency 1 V and 1000 Hz for resistance measurements.

The phase compositions of the hydration products were determined by X-ray diffraction using a Philips diffractorneter with a scanning speed of 1°2θ/min (Ni-filtered CuKa radiation). Differential scanning colorimetry runs were conducted using a Shimadzu type 50-thermal analyzer at a heating rate of 10 °C/min. The microstructure of the selected samples was examined using a high-resolution scanning electron microscope JEOL JXA-840.

3. Results and discussion

3.1. Electrical conductivity

Figs. 2–7 show the variations of electrical conductivity of CAC with curing temperature and slag content. When the CAC grains come into contact with water [1], three distinct reactions can be identified: dissolution, nucleation and precipitation. During the first period, dissolution of the cement particles bringing $Ca^{2+}$and $Al(OH)_4^-$ ions into solution takes place, and the electrical conductivity is increased. A small amount of hydrates will form at this stage where very slight changes of the electrical conductivity are detected. The dissolution will continue with a consequent increase in the concentration of $Ca^{2+}$and $Al(OH)_4^-$ ions until

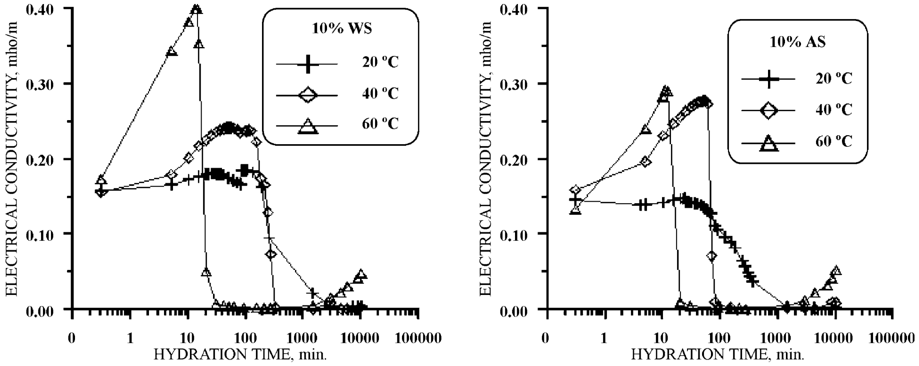

Fig. 4. Electrical conductivity of CAC containing 10 mass% of AS or WS at different temperatures.

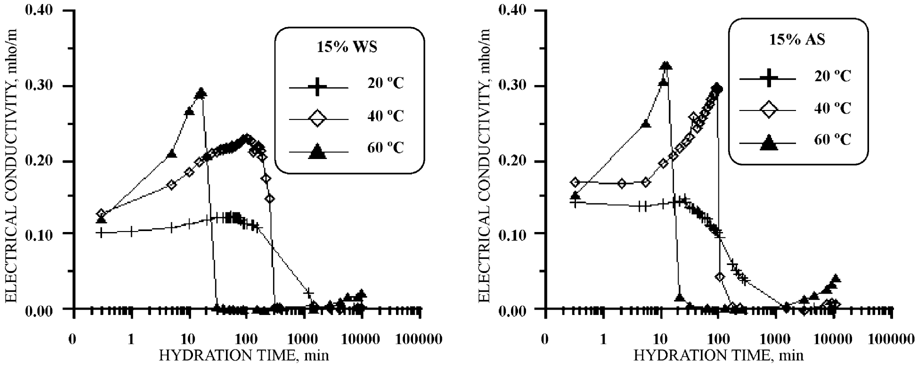

Fig. 5. Electrical conductivity of CAC containing 15 mass% of AS or WS at different temperatures.

a saturation point is reached. After the dissolution reaction, the nuclei are formed and grown to a critical size and quantity [16]. In the rapid precipitation of hydrates that follow, the electrical conductivity decreases promptly, consuming ions from the solution. This causes a drop in solution concentration, and the dissolution of the anhydrous CAC is accelerated (the electrical conductivity rises).

It is generally observed that the formed hydrates depend on the curing temperature. Four different types of hydrated phases can be present in the CAC; namely, CAH_{10}, C_2AH_8, C_3AH_6 and AH_3 formed according to the following reactions:

- At low temperature<15 °C, CAH_{10} is the main formed hydrate:

  $CA + 10H \rightarrow CAH_{10}$

- At temperature between 15 and 30 °C, CAH_{10} is precipitated together with C_2AH_8 and AH_3 gel:

  $2CA + 11H \rightarrow C_2AH_8 + AH_3$

- At temperature >30 °C, C_2AH_8 and AH_3 gel are formed together and converted rapidly, if not simultaneously above 45 °C into C_3AH_6 and AH_3 (gibbsite):

  $2CA + 12H \rightarrow C_3AH_6 + AH_3$

Fig. 2 shows the variation in electrical conductivity of neat CAC with curing temperatures for time up to 7 days (10,080 min). The electrical conductivity increases as hydration develops with the curing time to reach a conductivity maximum, then decreases. The solubility of CAH_{10} increases significantly with temperature thus making precipitation more difficult as the temperature increases. With increase of the temperature up to 27 °C, nucleation of this phase becomes increasingly difficult relative to C_2AH_8 [1]. As the curing temperature increases up to 40 °C, the electrical conductivity increases while it shows a broad peak as at 20 °C. This may be attributed to an increase of the nucleation time with CAH_{10}.

At 60 °C, the conductograms are similar in shape to those obtained at 20 and 40 °C, with two main differences: the intensity of the conductivity maximum is higher, and the conductivity maximum is shifted to shorter hydration times. These results can be attributed to the increase of both the degree of hydration of the anhydrous cement constituents and the rate of formation of hydration products upon increasing temperature. The crossing of the conductivity curves indicate that, in addition to their concentration, the mobility of ions represents an important factor in affecting the conductivity values. This result reflects the effect of the nature of pores in these samples on the mobility and therefore on the conductivity values. With increase of the curing temperature up to 60 °C, the hydration of CAC takes place very quickly; a maximum of conductivity occurs within the first 12 min, and then, it sharply decreases again.

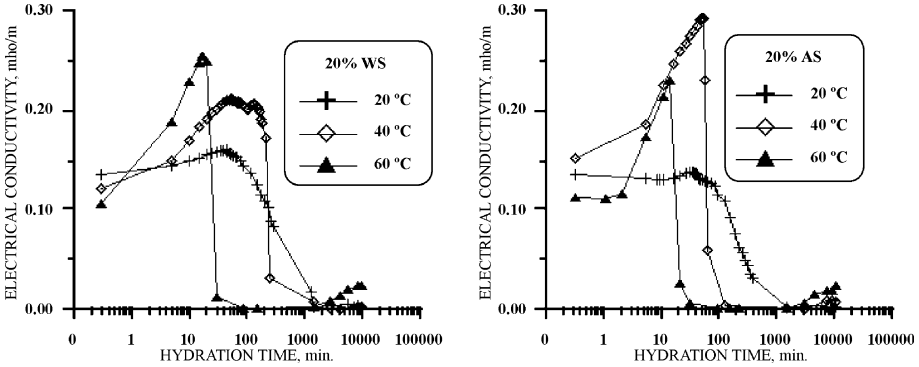

Fig. 6. Electrical conductivity of CAC containing 20 mass% of AS or WS at 20, 40 and 60 °C.

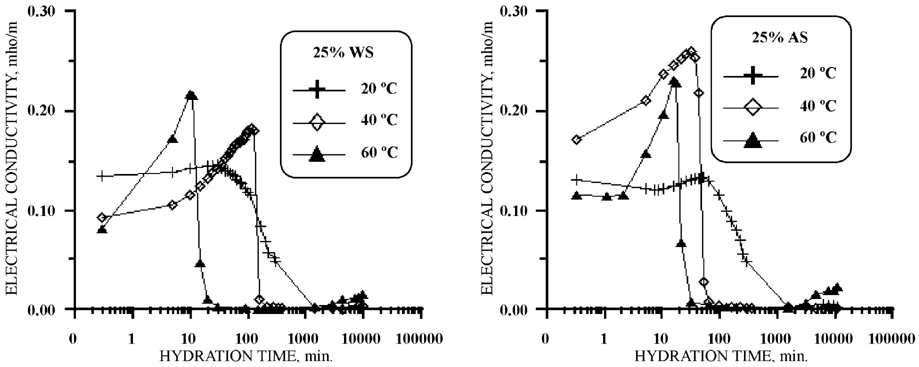

Fig. 7. Electrical conductivity of CAC containing 25 mass% of AS and WS at 20, 40 and 60 °C.

The results of Figs. 3–7 demonstrate the effect of slag content on the electrical conductivity values of the CAC/slag blend pastes. In general, the height of the first conductivity maximum decreases as the slag content increases (AS or WS). This is attributed to the hydration compounds precipitated due to the hydration of the slag portion as well as the reaction between the silica present in the slag portion to form stratlingite (C_2ASH_8), which will decrease the electrical conductivity values.

Edmonds et al., [17] showed that when water is added to CAC/slag mixtures; the first reaction is the hydration of CAC to produce hydrated calcium aluminates. The slag reacts slowly to give crystalline hydrates containing silica. The formation of C_2ASH_8 removes calcium ions from the pore solution and hence restricts the conversion of CAH_{10} and C_2AH_8 to the stable cubic hydrate C_3AH_6. The formation of C_2ASH_8 depends on the activation of the glassy slag to release silica; so, it seems that slag activation is enhanced by some of the minor phases in the commercial CAC, possibly the alkali metal hydroxides [18]. Fu et al. [19] consider that the slag acts as a inert microfiller in CAC, particularly at early ages.

WS (5–10%) gave higher electrical conductivity values than that containing AS at all curing temperatures. However, at 40 °C, the electrical conductivity values for pastes containing AS showed similar or higher values and shifted to a shorter hydration time. On increasing the slag content to 15–25 mass%, the electrical conductivity peak corresponding to AS was higher than WS and shifted to a lower hydration time. On increasing the temperature to 60 °C, the conductivity peaks shifted to a lower hydration time. On progressive hydration, the consumption of the ions increases, and more hydration products were formed; as a result, the conductivity values decrease sharply.

Fig. 8 shows the change of electrical conductivity of hydrated CAC and CAC containing 25 mass% of AS or WS and cured at different temperatures from 24 to 168 h. At 20 °C, the electrical conductivity of CAC decreases from 24 up to 72 h. After 72 h, there is no change in the electrical conductivity of CAC. Most hydration products are formed within the first 24 h. The product is strong and of a very dense solid cementicious matrix. Whereas, the electrical conductivity of CAC containing 25 mass% of AS or WS have nearly the same values for the whole period.

When the curing temperature was increased to 40 °C for CAC, an increase in electrical conductivity at 144 h (6 days) was detected.

The formed cement hydrates CAH_{10} and C_2AH_8 are metastable at 30 °C. In due course, they are converted into C_3AH_6. During the conversion process, the existing cement

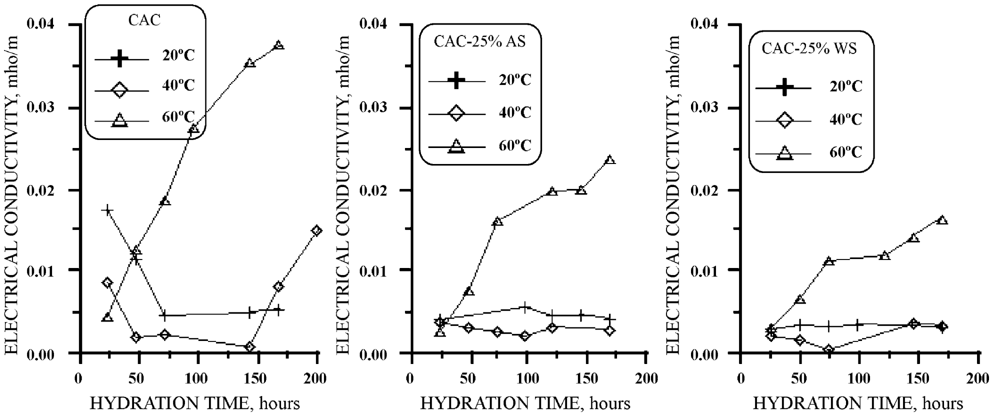

Fig. 8. Variation of electrical conductivity values of CAC and CAC containing 25 mass% of AS or WS curing at different temperature from 24 up to 168 h.

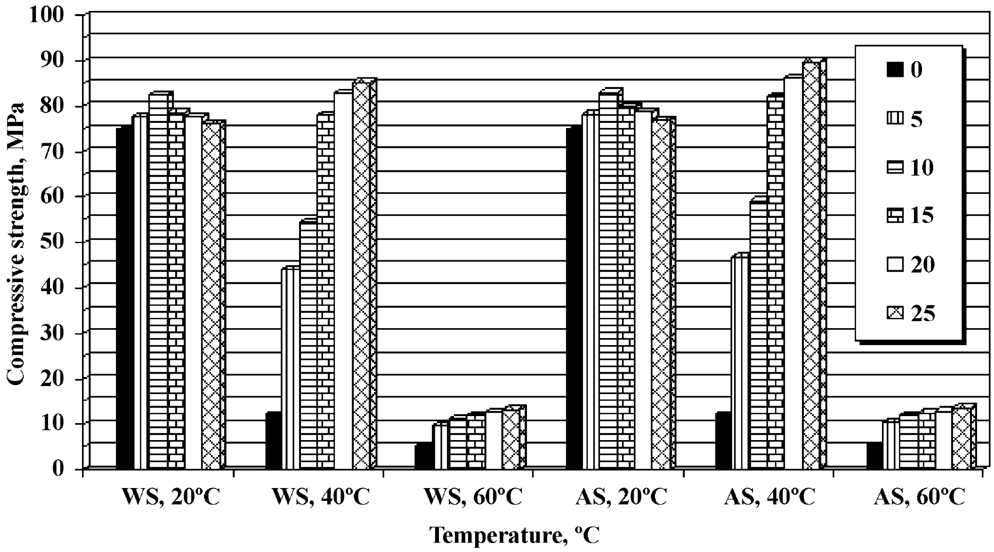

Fig. 9. Compressive strength of CAC and CAC containing AS or WS cured at 20, 40 and 60 °C at 60 days; first day cured at 20 °C.

hydrates CAH_{10} and C_2AH_8 release water, as shown in these two equations [20]:

$$3CAH_{10} \rightarrow C_3AH_6 + 2AH_3 + 18H$$

$$3C_2AH_8 \rightarrow 2C_3AH_6 + AH_3 + 9H$$

Water encourages future hydration, and the result is that the electrical conductivity of neat CAC increases significantly. At 40 °C, AS and WS prevent the conversion reactions by the preferential formation of C_2ASH_8 compared to that of C_3AH_6 [5]. The electrical conductivity of AS and WS were not changed at 40 °C up to 7 days (168 h).

On increasing the curing temperature to 60 °C, the electrical conductivity increases to reach a maximum within the first 12–20 min and then sharply decreases to constant values up to 24 h, as shown in Figs. 2–7, and then the electrical conductivity is sharply increased up to 168 h (Fig. 8). In the presence of AS and WS, the electrical conductivity is lower than that of CAC. It is therefore obvious that, at 60 °C, the addition of AS and WS effectively reduces the extent of conversion reactions. These results confirm the result obtained from DSC and XRD techniques, as shown later.

3.2. Compressive strength

The strength development of the investigated mixes at different temperatures seems to be related to the mineralogical transformation which takes place. Fig. 9 illustrates the compressive strength of neat CAC and CAC containing AS or WS cured at 20, 40 and 60 °C for 60 days. The compressive strength increases with the slag content up to 10 mass% at 20 °C. With the increase of the amounts of slag, the compressive strength showed a slight decrease but is still higher than that of neat CAC. The increase of the compressive strength is due to the formation of stratlingite instead of C_3AH_6 and the formation of CSH (II). At 40 °C, the compressive strength of CAC decreases from 74.5 at 20 °C to 12.0 MPa due to the conversion process. Addition of 5

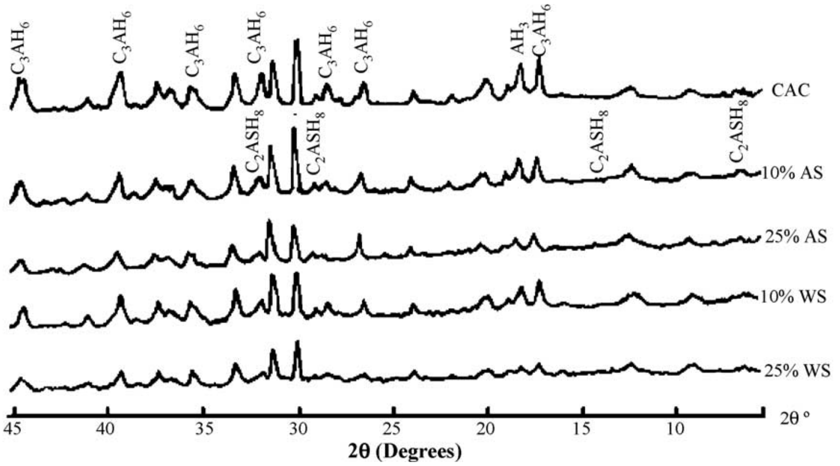

Fig. 10. XRD patterns of hydrated CAC and hydrated CAC-AS or CAC-WS pastes cured at 40 °C for 28 days.

mass% of either AS or WS slags increases the compressive strength to 46.8 and 44.1 MPa, respectively. At this temperature, the compressive strength increases with the slag content up to 25 mass% to become 89.7 and 85.2 MPa for AS and WS. This means that the increase in the curing temperature may enhance the hydration reaction of the slag as well as its reaction with the CAC-hydrated phases to form the more stable stratlingite compound, as will be seen later in XRD and DSC results, and this may compensate for the strength decline. As the curing temperature increase to 60 °C, the compressive strength decreases due to the conversion, which takes place at 1 day to produce C_3AH_6 in preference to CAH_{10} and C_2AH_8. The volume of the hydrates of CAH_{10} and C_2AH_8 are higher than that of C_3AH_6; the crystallization of C_3AH_6 having small volume leads to an increase in the apparent porosity, and consequently, the strength decreases. The compressive strength increases in the presence of slag AS or WS is due to the formation of stratlingite. Stratlingite is a stable crystalline phase in the temperature up to 70 °C [5]. In this system, AS has a hydraulic activity nearly the same as that of WS. At high temperatures, 40 and 60 °C, it gives higher strength than that with WS.

3.3. XRD

XRD patterns of hydrated CAC and CAC containing 10 and 25 mass% of AS and WS pastes cured under water at 40 °C up to 28 days are presented in Fig. 10. Hydrogarnet is the major hydrated cement phase in CAC pastes. Addition of slag (10 mass% of AS or WS) reduces the peak intensities of C_3AH_6 phase. Twenty-five mass% of AS or WS appears to be more effective in reducing the C_3AH_6 formation. However, it does not prevent the conversion completely; only small peaks of C_3AH_6 were detected in pastes containing 25 mass% of slag. Small peaks representing stratlingite found in CAC/slag pastes may be due to the encapsulation of the formed stratlingite compound by large quantity of AH_3 gel formed as a result of the conversion process.

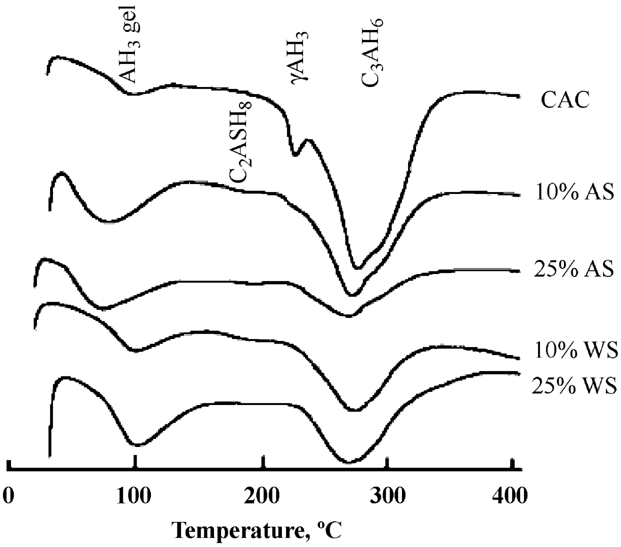

Fig. 11. DSC thermograms of CAC and M.10, M.25, C.10 and C.25 cured at 40 °C for 60 days.

Table 3
The enthalpy values of the characteristic endothermic peaks of gel and C_3AH_6 phases with temperatures, (J/g)

Mixture no.	70–100 °C	270–280 °C
M.0	34.51	240.50
M.10	84.51	178.87
M.25	124.94	109.70
C.10	68.89	168.00
C.25	91.45	119.10

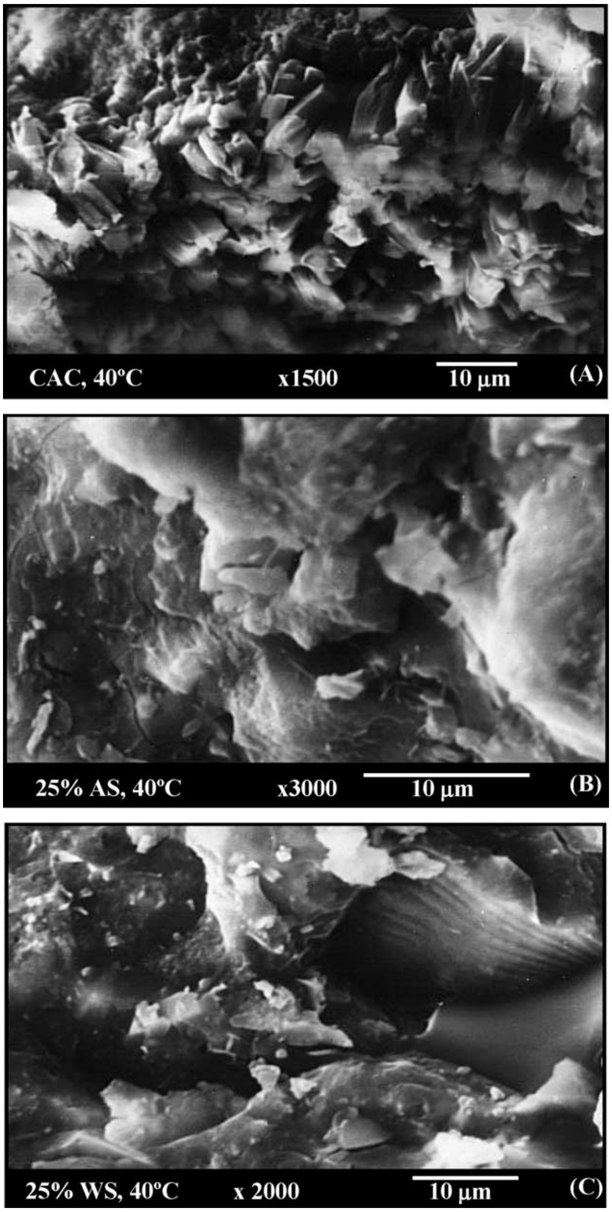

Fig. 12. SEM of hydrated CAC (A) and CAC containing AS (B) or WS (C) pastes cured at 40 °C for 60 days.

3.4. DSC

Fig. 11 depicts the DSC thermograms of hydrated CAC/slag pastes containing 10 and 25 mass% of AS and WS cured at 40 °C up to 60 days. The thermograms show four endothermic peaks located at 70–100, 160–180, 220–230 and 270–280 °C. The first endothermic peak is due to AH_3 gel. The endothermic peak located at 150–180 °C is attributed to the semicrystalline C_2AH_8. The broad endothermic band that occurs at 160–180 °C in CAC/slag is mainly due to C_2ASH_8. The third endothermic peak is due to gibbsite (γAH_3). The last endothermic peak is attributed to C_3AH_6. The enthalpies of endothermic peaks that are located at 270–280 and 70–100 °C are given in Table 3. It is clear from Table 3 that the addition of 10 mass% of AS (M.10) or WS (C.10) reduces the formation of C_3AH_6 by $\approx$26.3% and 30%, respectively. On the other hand, 25 mass% of AS (M.25) and WS (C.25) reduces the formation of C_3AH_6 by $\approx$54.6% and 50.4%, respectively. The great differences in the enthalpy values of the peak located at 70–100 °C for specimens containing AS and WS are due to the formation of CSH (II) as a result of the slag hydration reactions [21].

3.5. SEM

The morphology and microstructure of hydrated CAC and CAC pastes containing 25 mass% of AS or WS cured at 40 °C are depicted in Fig. 12. The micrograph in Fig. 12A shows the presence of cubic and granular crystals of C_3AH_6 as well as AH_3 gel, which could be detected in the upper part of the micrograph. The porous and weak structure may be responsible for the low strength. The microstructures shown in Fig. 12B and C illustrate the dense texture to which the strength improvement is related. Stratlingite phase was detected in this micrograph. Stratlingite (C_2ASH_8) was formed in significant quantities in preference to C_3AH_6. Fig. 12B and C show little amounts of amorphous gel materials located around the stratlingite phase.

4. Conclusions

(1) In hydrated CAC pastes containing AS and WS, the electrical conductivity maximum decreases as the slag content increases. This result is mainly attributed to the interaction of slag with Ca^{2+} ions released, leading to the formation of stratlingite (C_2ASH_8), which results in a corresponding decrease in the electrical conductivity values.

(2) At 40 °C, electrical conductivity of CAC increases after 144 h (6 days), whereas CAC containing 25 mass% of AS or WS have nearly the same values.

(3) The compressive strength increases with the slag content up to 10 mass% at 20 °C. On increasing the amounts of slag, the strength values show a slight decrease, but it is still higher than that of neat CAC. At 40 °C, the compressive strength increases with slag content. In this system, AS has a hydraulic activity nearly the same as WS. At high temperatures (40 and 60 °C), it gives higher strength than WS.

(4) Addition of slag (AS or WS) reduces the X-ray peak intensities of C_3AH_6 phase. It does not prevent the conversion, but it suppresses the hydrogarnet formation. Ten mass% of AS or WS reduces the formation of C_3AH_6 by $\approx$26.3% and 30%, whereas replacing the CAC with 25 mass% AS and WS reduces the formation of C_3AH_6 by $\approx$54.6% and 50.4%, respectively.

References

[1] K.L. Scrivener, A. Capmas, Calcium aluminate cements, in: P.C. Hewlett (Ed.), Chapter 13 in Lea's Chemistry of Cement and Concrete, John Wiley & Sons, New York, NY, 1998, pp. 709–778.

[2] K.L. Scrivener, H.F.W. Taylor, in: R.J. Mangabhari (Ed.), Microstructure Development in Pastes of a Calcium Aluminate Cement, Chapman and Hall, London, UK, 1990, pp. 41–54.

[3] H.G. Midgley, P.B. Rao, Formation of stratlingite $2CaO.SiO_2.Al_2O_3.8H_2O$ in relation to the hydration of high alumina cement, Cem. Concr. Res. 8 (1978) 169–172.

[4] S. Marcdargen, M. Testue, J.P. Bayoux, A. Mathieu, Hydration and strength of blends of CAC and silica fume and stability of hydrates, Proc. 9th, Inter. Congr. Chem. Cem., vol. 4, New Delhi Science and Technology, New Delhi, India, 1992, pp. 651–657.

[5] S. Bentsen, A. Seltvit, B. Sanderg, Effect of microsilica on conversion of high alumina cement, in: R.J. Mangabhai (Ed.), Calcium Aluminate Cement, Chapman and Hall, London, UK, 1990, pp. 294–319.

[6] A.J. Majumdar, R.N. Edmonds, B. Singh, Hydration of calcium aluminate in presence of granulated blast furnace slag, Calcium Aluminate Cements, Proc. Inter. Sym. Queen Mary and Westfield College, University of London, 9–11 July, Chapman and Hall, London, 1990, p. 259.

[7] Y. Fu, J. Ding, J.J. Beaudoin, Mechanism of stratlingite formation in high alumina cement–siliceous material systems, Proc. 2nd CANMET/ACI Inter. Sym., Las Vegas, USA, June 11–14, 1995.

[8] C.H. Fentiman, S. Rashid, J.P. Bayoux, A. Bonin, M. Testud, The effect of curing conditions on the hydration and strength development in Fondu: slag, in: R.J. Mangabhai (Ed.), Calcium Aluminate Cement, Chapman and Hall, London, UK, 1990, pp. 272–281.

[9] A. Capmas, D.M. Sorrentino, D. Damidot, Effect of temperature on setting times of calcium aluminate cements, in: R.J. Mangabhai (Ed.), Calcium Aluminate Cement, Chapman and Hall, London, UK, 1990, pp. 65–80.

[10] Th.A. Bier, A. Mathieu, B. Espinosa, J.R Bayoux, The use of conductimetry to characterize the reactivity of calcium aluminate cements, Proc. UNITECR'93, Am. Ceram. Soc, Westerville, OH, 1993.

[11] A. Mathieu, B. Espinosa, Electrical conductimetry to control LCC's, Proc. ALAFAR, 1994.

[12] S. Rashid, X. Turrillas, Hydration kinetics of $CaAl_2O_4$ using synchrotron energy-depressive diffraction, Thermochim. Acta 302 (1997) 25–34.

[13] T. Oztiirk, J. Rapoport, J.S. Popovics, S.P. Shah, Monitoring the setting and hardening of cement-based materials with ultrasound, Concr. Sci. Eng. 1 (1999) 83–91.

[14] N.Y. Mostafa, S.A.S. El-Hemaly, E.I. Al-Wakeel, S.A. El-Korashy, P.W. Brown, Characterization and evaluation of the hydraulic activity of some industrial by-products: II. Water-cooled slag and air-cooled slag, Cem. Concr. Res. 31 (2001) 467–474.

[15] M. Heikal, I. Aiad, I.M. Helmy, Portland cement clinker, granulated slag and by-pass cement dust composites, Cem. Concr. Res. 32 (2002) 1805–1812.

[16] T.J. Chotard, N. Gimet-Bréart, A. Smith, Y. El Hafiane, J.P. Bonnet, P. Abelard, Electrical characterization at high frequency (I MHz I 6 Hz) of an aluminous cement, Ann. Chim. Sci. Mater. 25 (2000) 197.

[17] R.N. Edmonds, A.J. Majumdar, The hydration of mixtures of monocalcium aluminate and blast furnace slag, Cem. Concr. Res. 19 (1989) 779–782.

[18] A.J. Majumdar, R.N. Edmonds, The hydration of calcium aluminate in presence of blast furnace slag, in: R.J. Mangabhai (Ed.), Calcium Aluminate Cement, Chapman and Hall, London, UK, 1990, pp. 259–271.

[19] Y. Fu, J. Ding, J.J. Beaudoin, Temperature dependence of compressive strength of conversion-inhibited high alumina cement concrete, ACI Mater. J. 94 (6) (1997).

[20] H.G. Midgley, High alumina cement in construction, a future based on experience, Proc. Inter. Symp., Calcium Alumina Cement, University of London, July 9–11, 1990.

[21] P.B. Rao, V.N. Viswanathan, Chemistry of arresting strength retrogression in structural high alumina cement, 7th Inter. Congr. Chem. Cem. Paris, vol. 5, Reu De Cronstadt, 75015, Paris, France, 1980, pp. 51–56.